Ghost Particle Velocimetry: Accurate 3D Flow Visualization Using Standard Lab Equipment

Stefano Buzzaccaro,* Eleonora Secchi, and Roberto Piazza
Department of Chemistry (CMIC), Politecnico di Milano, via Ponzio 34/3, 20133 Milano, Italy
(Received 14 March 2013; published 25 July 2013)

We describe and test a new approach to particle velocimetry, based on imaging and cross correlating the scattering speckle pattern generated on a near-field plane by flowing tracers with a size far below the diffraction limit, which allows reconstructing the velocity pattern in microfluidic channels without perturbing the flow. As a matter of fact, adding tracers is not even strictly required, provided that the sample displays sufficiently refractive-index fluctuations. For instance, phase separation in liquid mixtures in the presence of shear is suitable to be directly investigated by this ''ghost particle velocimetry'' technique, which just requires a microscope with standard lamp illumination equipped with a low-cost digital camera. As a further bonus, the peculiar spatial coherence properties of the illuminating source, which displays a finite longitudinal coherence length, allows for a 3D reconstruction of the profile with a resolution of few tenths of microns and makes the technique suitable to investigate turbid samples with negligible multiple scattering effects.

DOI: 10.1103/PhysRevLett.111.048101 PACS numbers: 87.64.M−, 42.25.Fx, 47.61.−k, 47.80.Cb

The increasing complexity of microfluidics chips and their widespread diffusion in academic and company research labs calls for plain, low-cost, and practical methods to quantitatively monitor the fluid flow in these devices. A well-established technique is particle tracking velocimetry (PTV), where the fluid is seeded with small particles and a 2D velocity field is obtained by tracking the individual particle motion. Individual tracking, however, requires particles large enough to be optically resolved, which may perturb the flow over spatial scales comparable, in microfluidics, to those of the investigated structures. This limitation can be overcome by resorting to more sophisticated methods such as microscale particle imaging velocimetry (μPIV), which exploits small fluorescent tracers that do not need to be individually resolved. In fact, μPIV is becoming a common tool in research labs because of the availability on the market of several turnkey systems and software [1,2]. However, μPIV instrumentation requires a rather expensive optical setup, usually including a pulsed laser source synchronized with a fast, high-resolution camera. In this Letter, we present a new technique, which we dub ''ghost particle velocimetry'' (GPV), exploiting as in μPIV subresolution tracers, but with the main advantage of requiring just a standard bright-field microscope with Köhler illumination. Because of the peculiar spatial coherence properties of the illumination source, which can be easily tuned by operating on the condenser field diaphragm, this technique, besides providing a good resolution of the transversal (in-plane) flow field, allows for an appreciable longitudinal resolution along the optical axis. In addition, GPV has weak requirements concerning the optical properties and concentration of the tracers: As a matter of fact, adding tracers may not even be required in the presence of sufficiently strong intrinsic refractive-index fluctuations in the sample. This feature makes GPV particularly suitable for investigating the flow properties of emulsions, or fluid mixtures and liquid crystals close to a phase transition, where the addition of colloidal tracers might be problematic, if not unfeasible.

The method we propose relies on a promising combination of standard microscope imaging with novel ideas that widely extend the potential of a well-established intensity correlation technique, dynamic light scattering (DLS) [3]. Video microscopy, suitable for optically resoluble objects, and DLS, where subresolution particles are investigated by quantifying their Brownian diffusion from the time correlation of the scattered intensity, have long been among the most powerful techniques for particle sizing. They also allow us to perform velocimetry studies: Whereas standard PTV relies on microscope imaging, the motion of subresolution particles can indeed be obtained by Doppler velocimetry, a heterodyne DLS technique where the scattered field ''beats'' with a fraction of the incident beam. While these two approaches are generally considered as distinct and complementary, clever optical schemes, bridging the gap between scattering and imaging approaches, have recently been proposed [4]. The basic strategy shared by these novel techniques consists in collecting the light scattered by the sample within the so-called ''deep Fresnel'' region, corresponding to near-field (NF) diffraction [5]. This allows getting information on the sample structure and dynamics equivalent to that provided by DLS in the far field, with the crucial advantage of simultaneously retaining spatial resolution. Conceptually and chronologically, the first of these techniques is heterodyne near-field scattering (HNFS), which consists in sending a spatially filtered and expanded laser beam with wavelength λ through a cell filled with a particle dispersion and detecting the scattered intensity distribution of the speckle pattern on a plane at close distance z from the sample,

possibly magnified by a collection optics, with a CCD/CMOS multipixel sensor [6]. Within a suitably defined distance range, the angular spectrum component at wave vector q of the scattered radiation superimposes with the transmitted beam; hence, HNFS is basically a heterodyne technique where the transmitted field E_0 plays the role of local oscillator. Provided that the scattered field E_s is much weaker than E_0, the intensity at a point $\mathbf{x}$ on the detection plane is given by

$$I(\mathbf{x}, t) = |E_0 + E_s(\mathbf{x}, t)|^2 = I_0 + 2\mathrm{Re}\{E_s(\mathbf{x}, t)E_0^*(\mathbf{x})\}. \quad (1)$$

On top of the strong contribution I_0 coming from the transmitted beam, this NF intensity pattern displays therefore a much milder modulation in the form of a random interference speckle pattern, which can be brought out by subtracting the time-independent background contribution I_0, obtained as the average intensity of many statistically independent images. Very interestingly, in the simplest case of a suspension of noninteracting colloidal particles, the statistical size of a NF speckle coincides with the size of the scattering particles. More generally, a suitable extension of the van Cittert–Zernicke theorem allows us to relate the mutual intensity on the detection plane $J(\mathbf{x}_1, \mathbf{x}_2) = \langle E(\mathbf{x}_1, t)E^*(\mathbf{x}_2, t)\rangle$ to the Fourier transform of the intensity pattern measured by standard light scattering in the far field [7]. Hence, in a heterodyne detection scheme, the Fourier transform of the normalized intensity fluctuations $i(\mathbf{x}, t) = [I(\mathbf{x}, t) - I_0]/I_0$ on the detection plane is proportional to the structure factor of the sample. The time dynamics of each single NF speckle is related to the Brownian dynamics of the scatterers through a superposition of decay modes at different scattering wave vectors q, which can be set apart by Fourier analysis [4,6]. In addition, when the scatterers move coherently, the speckle pattern drifts according to the local flow pattern, making HNFS suitable to be used as a flow-mapping technique even if the scatterers are too small to be optically resolved [8].

In its original configuration, HNFS exploits a monochromatic, spatially coherent laser source. In the past few years, however, seminal investigations aimed to extend HNFS to the x-ray domain have shown that both temporal and spatial source coherence requirements can be largely relaxed [4,9]. Since in NF conditions the speckle patterns corresponding to different wavelengths superimpose to a good degree of accuracy, monochromaticity is indeed not an issue, and the simple lamp or condenser illumination optics of a standard bright-field microscope is fully adequate. In a Köhler illumination scheme, where the source plane is conjugated with the aperture diaphragm, the source étendue (the product of its size times its diverging angle) can easily be tuned by opening or stopping down the condenser. This is the principle of a powerful technique known as differential dynamic microscopy (DDM) [10]. Whereas in standard microscopy one usually works with a fully open condenser to maximize resolution by means of a spatially incoherent illumination, in DDM the source coherence area on the sample plane is effectively controlled by tuning the condenser numerical aperture NA_c. When the condenser is fully stopped down, so that the illumination is spatially coherent over the whole sample area, DDM and HNFS are conceptually equivalent; however, with partially coherent illumination, DDM presents crucial advantages that we shall discuss.

Ghost particle velocimetry exploits a DDM scheme to quantitatively map fluid flow in microfluidic devices using as tracers nanometric size scatterers. The basic idea of the technique is the following. Consider a suspension of particles lying within a thin layer perpendicular to the microscope optical axis and undergoing uniform motion with in-plane constant velocity $\mathbf{V}$. Neglecting the effect of particle Brownian motion, the NF speckle pattern generated by the suspension at time $t + \Delta t$ is then obtained from the pattern at time t with a simple spatial translation by $V\Delta t$ along the flow direction. Hence, the time-correlation function of the normalized intensity [11] $G_{\mathbf{x},t}(\Delta t; \Delta\mathbf{x}) = i(t, \mathbf{x} + \Delta\mathbf{x})i(t + \Delta t, \mathbf{x} + \Delta\mathbf{x})$, when mapped as a function of the displacement vector $\Delta\mathbf{x}$, displays a well-defined peak at $\Delta\mathbf{x} = \mathbf{V}\Delta t$, and the flow velocity can be readily obtained from the shift of such a cross-correlation peak between different images. On top of this uniform shift, Brownian agitation just induces a progressive broadening and decay of the amplitude of the cross-correlation peak, which can be used to estimate diffusion coefficient of the tracers [12,13]. The crucial advantage of GPV with respect to PIV methods can easily be spotted by recalling that the size of the NF speckles generated by subwavelength independent scatterers is ultimately determined only by the angular acceptance of the collection optics. Since extracting the velocity field requires one only to follow the speckle motion, the tracer size plays a little role. What is mainly required is that the tracers scatter sufficient light; thus, using particles with a high refractive index contrast with the solvent is advisable.

Our setup consists of a standard Olympus BX61 microscope equipped with long working distance objectives. Sample images are acquired with a simple CCD camera (Pike Allied Vision, 12 bit, 640×480 pixels 7.4×7.4 μm in size). Suspensions of polystyrene particles with a radius $R \simeq 40$ nm are flown though simple polydimethylsiloxane microfluidic channels prepared by standard soft lithography. A typical run consists of a sequence of 1000–4000 images, acquired with a frame rate of 200–400 frames/s, an exposure time of a few milliseconds, and a condenser numerical aperture set between $0.10 < NA_c < 0.15$. In bright-field images, the particle scattering contribution is basically masked by the strong background due to the transmitted beam and further disturbed by the occurrence of diffraction spots due to the presence of dust on the camera and optical components. However, a well-defined speckle pattern becomes manifest

by simply subtracting out the background static contribution, obtained as the average of a large number of successive frames, while at the same time spurious contributions cancel out. The flow reflects into an uniform motion of this speckle pattern, which can be appreciated in the movie MOV1 included as Supplemental Material [14], showing a suspension flowing in a channel of depth 600 μm, with focus on the channel midplane. Since the flow is stationary, the fluid motion can be quantitatively monitored by cross correlating each image in a run with the image m frames apart, time-averaging the results. Figure 1 (left panel) shows the cross-correlation maps between images separated by $m = 1, 3, 5$ frames, where the flow velocity can be easily obtained from the correlation peak displacement with respect to the center of the correlation map. The right panel shows that the peak amplitude decreases with m as a result of the progressive loss of correlation due to particle Brownian motion. The speckle pattern analysis can be performed by minimally adapting standard μPIV algorithms [15].

More interesting is of course probing a stationary, but spatially nonuniform flow pattern. A coarse-grained velocity field can in this case be extracted by splitting the images in a set of square "regions of interest" (ROIs) and analyzing the time behavior of the spatial cross-correlation function within each ROI. As a simple example, we have analyzed the flow profile within a channel 100 μm wide and 30 μm deep, in the presence of simple triangular obstacles obstructing the flow (Fig. 2). Since the flow stationarity allows for averaging over a large number of frames, the size of a ROI can actually be taken as small as the region on the image corresponding to a single pixel on the sensor, which yields very good spatial resolution. The inset in Fig. 2 shows the correlation maps for several single-pixel ROIs, placed just in front of the obstacle, obtained with a time averaging of about 10 s (4000 frames at 381 frames/s). Analyzing the shift of the cross-correlation peaks allows us then to reconstruct the local displacement field.

A crucial advantage in using a DDM scheme instead of exploiting a coherent source with a NFS setup comes out if we observe that, quite often, a real sample can hardly be regarded as an infinitely thin layer, as we did to introduce the GPV technique. Hence, the light collected by the sensor comes not only from the plane in focus but rather from a 3D region with a transverse depth that depends on collection optics and illumination characteristics. For fluorescent tracers, emitting incoherently, this "depth of correlation" (DoC) is essentially determined by the depth of field of the objective lens [1,2], but when the signal comes from scattering, the *longitudinal* spatial coherence of the source plays a major role [16]. With a laser source with a very long longitudinal coherence length, the *whole* sample contributes to the image formation. When the flow velocity varies along the optical axes, however, the weighted average of the velocity distribution inside the sample yields a distorted correlation peak with a "cometlike" shape [8] that biases the velocity field reconstruction and does not allow for sectioning the flow pattern along z. Stopping down the condenser, as made in DDM, conversely amounts to illuminating the sample with a "mosaic" of independent coherence areas with transverse dimension $\delta x \sim \lambda/NA_c$ [17]. These coherence "patches," however, have also a finite *longitudinal* size $\delta z \sim \lambda/(NA_c)^2$: Hence, the partial coherent illumination used in DDM probes only a finite sample region, approximately given by the 3D cigar-shaped coherence volume of the source, so that the heterodyne detection in Eq. (1) holds separately for each patch. For a microscope lamp with mean wavelength $\lambda \sim 500$ nm with NA_c set at 0.15, this effective DoC is $\delta z \sim 20$ μm [18]. With these settings, we investigated the 3D velocity field in a straight channel 600 μm deep, performing a z

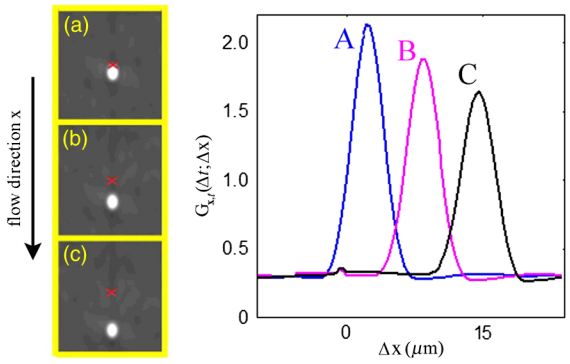

FIG. 1 (color online). Left panel: Average of 1000 cross correlation between images taken 1 (A), 3 (B), and 5 (C) frames apart at 200 frames/s. The red crosses indicate the origin of the correlation map. Right panel: Cross section of the three correlation peaks.

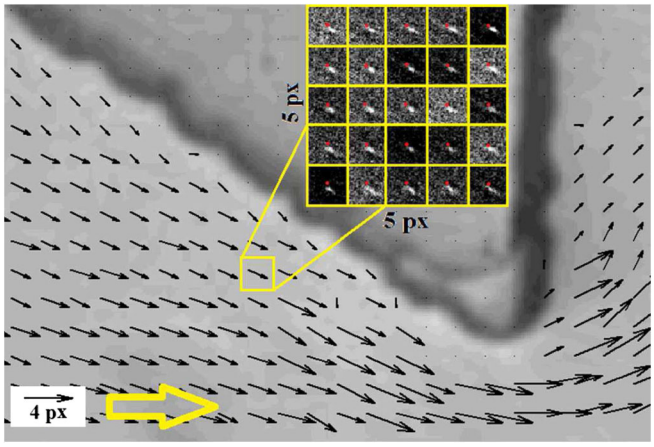

FIG. 2 (color online). Correlation maps and flow reconstruction around a simple obstacle in a microfluidic channel. The flow direction is shown by a yellow arrow. The maximal velocity at the channel narrowing corresponds to a Reynolds number Re $\simeq 5 \times 10^{-2}$.

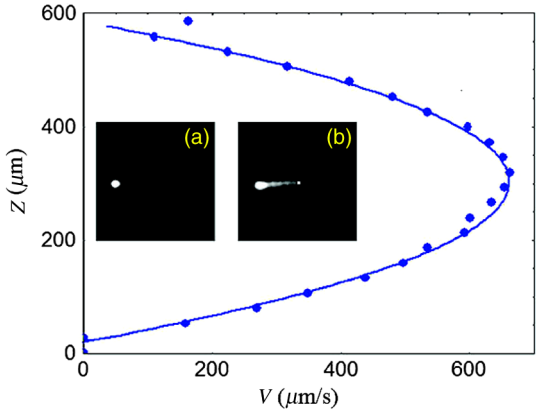

FIG. 3 (color online). Main body: z-scan longitudinal flow pattern in a straight channel, with the full line showing the predicted parabolic flow. The correlation map obtained at a depth $z = 300$ μm in a 600 μm deep channel is shown in inset (a). Inset (b) conversely shows that the correlation map obtained in a 30 μm deep channel displays a "comet" effect similar to what is observed in velocimetry methods using a laser source.

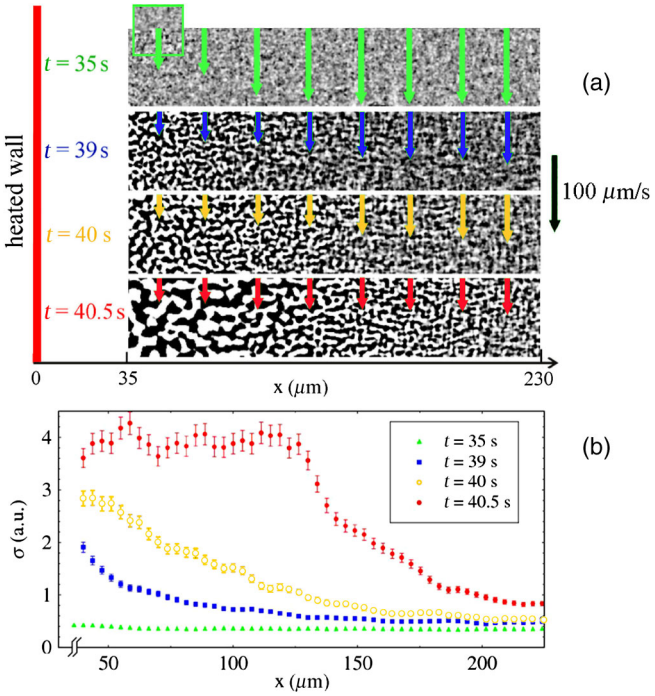

FIG. 4 (color online). Spinodal decomposition of a C10E5 +water mixture, prepared at the critical surfactant concentration $c \simeq 3.5\%$ by weight and fed into a 4 mm $\times$ 0.2 mm glass capillary at constant pressure head $\Delta P = 10^2$ Pa at an initial temperature distance $T_c - T \simeq 5°$ from the critical point. Ohmic heating is provided by a resistor thermally contacted to a metal block attached to the left cell wall. Panel (a): Speckle and flow velocity patterns at diverse heating times. The box at the top left indicates the size of the region where averaging was performed to obtain the locally averaged flow speed $\bar{V}(x)$ indicated by the arrows. Note that, at constant pressure head, $\bar{V}(x)$ decreases by more than a factor of 3 from the homogeneous to the phase-separated state, indicating a consistently higher effective viscosity of the latter. Panel (b): Time evolution of the standard deviation of the speckle patterns as a function of the distance from the heated wall.

scan with longitudinal steps of 20 μm. The results are summarized in Fig. 3, where the results of the correlation analysis are compared to the theoretical parabolic flow profile. Figure 3(b) conversely shows that the cross-correlation peak obtained for a shallower channel, where the velocity varies appreciably over distances shorter than δz, displays the cometlike shape typical of coherent laser probing. Thus, with some trade-off of spatial resolution, z scans usually performed by sophisticated techniques such as confocal differential dynamic microscopy [19] can be obtained by GPV with high speed.

Finally, we stress again that the GPV approach may not even require adding tracer particles on purpose: Structured complex fluids like emulsions, of primary importance in food and drug engineering, can often be studied in their natural, unaffected form. MOV2 in the Supplemental Material [14] shows, for instance, the flow in a microfluidic channel of skimmed milk, which is a dispersion of droplets with an average size (obtained by DDM) of about 280 nm, hence barely resolvable in bright field or even phase contrast microscopy. The sample may not even have a particulate structure, provided that it displays sufficiently strong intrinsic refractive index fluctuations. A physical meaningful example is provided by MOV3 of the Supplemental Material [14], which shows the progressive transition of an aqueous micellar solution of the nonionic surfactant C10E5 (pentaethyleneglycol monodecyl ether) from a homogeneous phase to a spinodal-decomposed mixture, when brought within the coexistence curve by transversally heating the sample from a wall. Note that a well defined speckle pattern is already evident in the *single phase* region (first 4 s of movie MOV3), even if the basic constituents of the mixture are globular micelles with a size of a few nanometers, due to the presence of strong critical fluctuations close to the critical temperature. Although this is evidently a case of a nonstationary flow, reasonable statistics can be obtained by using a high frame rate (170 frames/s) that allows time averaging with a window of about 50 ms, over which the speckle pattern shows negligible changes. Figure 4, for instance, shows that the standard deviation σ of the speckle pattern considerably grows as the heating time goes by, reflecting the progressive birth of the two phases from the wall. Since σ is directly related to the amplitude of the local concentration fluctuations, these preliminary results suggest GPV as an useful technique to investigate the effect of shear on phase separation.

We thank R. Cerbino, L. Cipelletti, and M. D. Alaimo for useful discussions. S. B. acknowledges funding by the Italian Ministry of Education and Research ("Futuro in Ricerca" Project Anisoft/RBFR125H0M).

*stefano.buzzaccaro@polimi.it

[1] R. Lindken, M. Rossi, S. Große, and J. Westerweel, Lab Chip **9**, 2551 (2009).
[2] S. T. Wereley and C. D. Meinhart, Annu. Rev. Fluid Mech. **42**, 557 (2010).
[3] B. Berne and R. Pecora, *Dynamic Light Scattering* (Wiley, New York, 1970).
[4] R. Cerbino and A. Vailati, Curr. Opin. Colloid Interface Sci. **14**, 416 (2009).
[5] Which is still much farther from the sample, however, than the region where evanescent waves still contribute, probed by scanning near-field optical microscopy.
[6] F. Ferri, D. Magatti, D. Pescini, M. A. C. Potenza, and M. Giglio, Phys. Rev. E **70**, 041405 (2004).
[7] R. Cerbino, Phys. Rev. A **75**, 053815 (2007).
[8] M. D. Alaimo, D. Magatti, F. Ferri, and M. A. C. Potenza, Appl. Phys. Lett. **88**, 191101 (2006).
[9] R. Cerbino, L. Peverini, M. A. C. Potenza, A. Robert, P. Bösecke, and M. Giglio, Nat. Phys. **4**, 238 (2008).
[10] R. Cerbino and V. Trappe, Phys. Rev. Lett. **100**, 188102 (2008).
[11] For a generic flow pattern, $G_{\mathbf{x},t}$ depends in principle on both the location x and the initial time t. In the stationary flow regimes, data statistics is, however, considerably improved by averaging over many time frames.
[12] M. G. Olsen and R. J. Adrian, Opt. Laser Technol. **32**, 621 (2000).
[13] L. Cipelletti, G. Brambilla, S. Maccarrone, and S. Caroff, arXiv:1306.4073.
[14] See Supplemental Material at http://link.aps.org/supplemental/10.1103/PhysRevLett.111.048101 for the three movies on fluid flow visualization with additional DDM results.
[15] M. Stanislas, K. Okamoto, C. Kähler, J. Westerweel, and F. Scarano, Exp. Fluids **45**, 27 (2008).
[16] F. Giavazzi, D. Brogioli, V. Trappe, T. Bellini, and R. Cerbino, Phys. Rev. E **80**, 031403 (2009).
[17] A. Gatti, D. Magatti, and F. Ferri, Phys. Rev. A **78**, 063806 (2008).
[18] The DoC which can be attained by opening up the condenser, however, has a practical lower limit, since the speckle contrast reduces by increasing NA_c, becoming negligible for $NA_c > 0.3$.
[19] P. J. Lu, F. Giavazzi, T. E. Angelini, E. Zaccarelli, F. Jargstorff, A. B. Schofield, J. N. Wilking, M. B. Romanowsky, D. A. Weitz, and R. Cerbino, Phys. Rev. Lett. **108**, 218103 (2012).